Journal of Inflammation Research

Dovepress
Taylor & Francis Group

Open Access Full Text Article

ORIGINAL RESEARCH

Lipoxin A4 Attenuates *E. coli*-Induced ARDS-Like Lung Injury in Mice via ALX/FPR2-Dependent Macrophage Reprogramming

Bingxue Zhang[1,2,*], Meng Xu[1,3,4,*], Yanling Deng[5,*], Donghui Li[5], Jun Shen[1,3], Chun Pan[1,5], Hongli He[1,5,6]

[1]Department of Critical Care Medicine, Sichuan Academy of Medical Sciences, Sichuan Provincial People's Hospital, Chengdu, Sichuan, 610031, People's Republic of China; [2]School of Medicine and Life Sciences, Chengdu University of Traditional Chinese Medicine, Chengdu, Sichuan, 610031, People's Republic of China; [3]School of Clinical Medicine, Qinghai University, Xining, Qinghai, 810000, People's Republic of China; [4]Department of Critical Care Medicine, Affiliated Hospital of Xuzhou Medical University, Xuzhou, Jiangsu, 221000, People's Republic of China; [5]School of Medicine, University of Electronic Science and Technology of China, Chengdu, Sichuan, 611731, People's Republic of China; [6]Department of Intensive Care Unit, Sichuan Provincial People's Hospital Pujiang Hospital - Pujiang People's Hospital, Chengdu, Sichuan, 611630, People's Republic of China

*These authors contributed equally to this work

Correspondence: Hongli He; Chun Pan, Department of Critical Care Medicine, Sichuan Academy of Medical Sciences, Sichuan Provincial People's Hospital, No. 32, West Section 2, First Ring Road, Chengdu, Sichuan, 610031, People's Republic of China, Email hhl0408@163.com; panchun1982@gmail.com

Background: Acute respiratory distress syndrome (ARDS) remains a severe inflammatory lung disorder with limited disease-modifying therapies. Lipoxin A4 (LXA4) is an endogenous specialized pro-resolving mediator that can modulate macrophage responses; however, its role in bacterial ARDS-like injury and the underlying ALX/FPR2-associated mechanism remain incompletely defined. To determine whether post-injury LXA4 attenuates *Escherichia coli* (*E. coli*)-induced ARDS-like lung injury in mice and whether these effects are associated with ALX/FPR2-dependent macrophage reprogramming.

Methods: Male C57BL/6J mice were randomized to PBS, ARDS, LXA4, or LXA4 + WRW4 groups (n=6 per group per time point). Mice were challenged intratracheally with *E. coli* (2 × 10^6 CFU in 50 μL) and treated 4 h later with intravenous LXA4 (7 μg /kg), with or without intraperitoneal WRW4 (1.8 mg/kg) administered at the time of LXA4 dosing. Bronchoalveolar lavage fluid (BALF), plasma, and lung tissue samples were collected at 24 h and 72 h for histology, injury scoring, BALF protein, bacterial burden, cytokine and lipid mediator ELISA, ROS, and HO-1 analyses. In vitro, MH-S alveolar macrophages were stimulated with LPS (1 μg/mL) and treated with LXA4 (200 nM), with or without WRW4 (10 μM), to assess cytokine secretion, STAT1/STAT3 expression, iNOS/CD206 markers, and cell-associated GFP-*E. coli* uptake.

Results: LXA4 reduced macroscopic and histological lung injury, the lung wet weight-to-body weight ratio, BALF IL-6, IL-1β and TNF-α levels, BALF protein leakage, and BALF bacterial burden after *E. coli* challenge. LXA4 also increased circulating LXA4 while decreasing LTB4, LTC4, and PGE2, reduced lung ROS, and enhanced HO-1 expression. In MH-S cells, LXA4 decreased pro-inflammatory cytokine release, increased IL-10, promoted an M2-like marker profile, and enhanced cell-associated GFP-*E. coli* uptake. WRW4 attenuated these effects, supporting pharmacological involvement of ALX/FPR2 signaling.

Conclusion: LXA4 alleviates bacterial ARDS-like lung injury in mice and promotes pro-resolving macrophage features, with effects attenuated by ALX/FPR2 antagonism. These findings support LXA4/ALX-FPR2 signaling as a preclinical pro-resolving strategy that warrants validation in cell-specific and clinically representative ARDS models.

Keywords: acute respiratory distress syndrome, ALX/FPR2 receptor, inflammation resolution, lipoxin A4, macrophage reprogramming

Introduction

Acute lung injury (ALI)/acute respiratory distress syndrome (ARDS) represents a severe, life-threatening pulmonary condition with persistently high clinical mortality rates approaching 50%.[1,2] Survivors often suffered long-term

https://doi.org/10.2147/JIR.S597266
Received: 12 February 2026
Accepted: 25 June 2026
Published: 16 July 2026

complications, such as pulmonary fibrosis and impaired lung function, which profoundly compromise quality of life.[3,4] The pathogenesis of ARDS is multifactorial. Infectious and non-infectious insults activate resident and recruited immune cells, promote release of cytokines and chemokines, disrupt endothelial and epithelial integrity, and amplify oxidative and metabolic injury.[5,6] In infection-driven ARDS, therapy is particularly challenging because excessive inflammation must be restrained without impairing pathogen clearance;[7] therefore, pro-resolving strategies that preserve host defense are of particular translational interest.

Alveolar macrophages serve as the frontline defenders in lung tissue and pivotal initiators of inflammatory cascades, playing a central role in the progression of ALI/ARDS.[8,9] Alveolar macrophages exhibit two primary polarization programs—pro-inflammatory M1-like and anti-inflammatory/pro-resolving M2-like states, with imbalances favoring M1-like activation contributing to ARDS progression.[10,11] Upon pathogen invasion, pathogen-associated molecular patterns (PAMPs) and damage-associated molecular patterns (DAMPs) engage Toll-like receptors (TLRs) on resident macrophages, steering them toward the M1-like pro-inflammatory profile.[8,12,13] M1-like macrophages combat microbes by direct engulfment, secretion of TNF-α, IL-1β, IL-6 and related mediators, and release of chemokines to recruit circulating monocytes and lymphocytes; they also present antigens to activate T and B cells, amplifying antimicrobial defense.[2] Under the influence of the injury milieu and resolving cytokines, macrophages can transition to the M2-like anti-inflammatory state, producing IL-4, IL-10, and other suppressive factors to dampen excessive inflammation, scavenge debris and apoptotic cells, and foster tissue repair, angiogenesis, and fibrosis.[8,14,15] Consequently, strategies to restore macrophage functional balance and encourage pro-resolving shifts emerge as viable therapeutic avenues for ARDS.[16,17]

Lipoxins (LXs), derived from arachidonic acid via lipoxygenase-mediated transcellular biosynthesis, function as endogenous regulatory molecules in inflammation;[18] among them, lipoxin A4 (LXA4) is a key specialized pro-resolving mediator.[19] LXA4 promotes M2-like macrophage features and enhances efferocytosis, accelerating inflammation resolution and tissue restoration.[18,20] ALX/FPR2 is a major receptor mediating the pro-resolving actions of LXA4 and related mediators across inflammatory cells, airway and alveolar epithelium, and stromal compartments in the lung.[21–23] Upon activation by pro-resolving ligands such as LXA4, resolvin D1, and annexin A1, ALX/FPR2 generally restrains neutrophil-dominated inflammation, enhances macrophage-mediated clearance of apoptotic cells, supports epithelial repair, and attenuates profibrotic remodeling.[21–23] Existing evidence indicates that LXA4 interacts with the ALX/FPR2 to orchestrate immune responses and inflammation control:[21,24,25] this interaction not only refines macrophage activity and boosts phagocytosis,[26,27] while also alleviating inflammation and oxidative stress.[28] Nevertheless, it remains largely unclear how LXA4 concurrently regulates bacterial clearance, systemic lipid mediator profiles, macrophage activity, and oxidative stress in bacterial ARDS-associated injury. Pharmacological antagonism with WRW4 provides a useful approach to test receptor involvement, although it cannot by itself define cell-specific receptor contributions.[21]

Escherichia coli (*E. coli*) is a common pathogen of infection-associated ARDS, and an *E. coli*- induced model is well suited for investigating the balance between inflammation resolution and bacterial clearance.[7] We hypothesized that post-injury LXA4 administration would attenuate *E. coli*-induced ARDS-like lung injury by engaging ALX/FPR2-associated pro-resolving signaling, thereby reducing inflammatory and oxidative injury while supporting macrophage-mediated bacterial handling. To test this hypothesis, we used an *E. coli*-induced murine ARDS-like model and a lipopolysaccharide (LPS)-stimulated MH-S alveolar macrophage model with WRW4 antagonism. We measured lung histology, edema, BALF protein, cytokines and bacterial burden, plasma lipid mediators, lung ROS and HO-1, macrophage STAT1/STAT3 expression, iNOS/CD206 phenotype markers, cytokine secretion, and cell-associated bacterial uptake at early and later injury phases.

Material and Methods

Reagents

E. coli (ATCC 25922), GFP-expressing *E. coli* (ATCC 25922GFP) and MH-S cells (CRL-2019) were sourced from the American Type Culture Collection. Lipopolysaccharide (LPS; *E. coli* O55:B5), and the BCA protein assay kit were supplied by Shanghai Beyotime Biotechnology. qPCR primer pairs for mouse STAT1, STAT3, and the β-actin reference gene were synthesized by Chengdu Chuangnuofei Biotechnology. LXA4 (HY-113509) and WRW4 (HY-P1119) were purchased from MedChemExpress. ELISA kits for mouse LXA4 (JM-13196M1), LTB4 (JM-02324M1), LTC4 (JM-

02678M1) and PGE2 (JM-02345M1) were provided by Jiangsu Jingmei Biotechnology. IL-1β (422,321–003), TNF-α (424,582–011), IL-6 (423,914–004), IL-10 (423,914–005) and HRP-conjugated secondary antibody (31460) were obtained from Thermo Fisher Scientific. The reactive oxygen species (ROS) assay kit (E004-1-1) was obtained from Nanjing Jiancheng Bioengineering Institute. Antibodies against heme oxygenase-1 (HO-1) (10,701-1-AP) were purchased from Wuhan Sanying Biotechnology. iNOS (ER1706-89) and CD206 (ET170204) was obtained from Hangzhou HuaAn Biotechnology.

Animals

Specific pathogen-free male C57BL/6J mice (6–8 weeks old, 18–22 g) were obtained from Chengdu Dashuo Experimental Animal Co., Ltd. (SCXK(Chuan) 2020–0030), and maintained under standardized conditions (22–25 °C, 50–60% humidity) with a 12 h light/dark cycle and ad libitum access to food and water. Soft bedding and small plastic toys were provided to meet the needs of the mice's exploratory behavior and physiological activities.

Mice were randomly divided into four experimental groups (1:1:1:1) using a computer-generated random number sequence: PBS control, ARDS model, LXA4 treatment, and LXA4 + WRW4. The sample size was selected based on prior ALI/ARDS and LXA4 studies and feasibility considerations for detecting large treatment effects in prespecified injury and inflammation endpoints,[14,18] A formal a priori power calculation was not performed and is acknowledged as a limitation. A total of 96 mice were used. Two independent in vivo cohorts were established to avoid interference between BALF collection and lung-tissue analyses. Cohort 1 was used for BALF/plasma endpoints and Cohort 2 for histology and lung-tissue molecular assays. Each cohort included four groups and two time points, with n=6 mice per group per time point; therefore, 48 mice were included in each cohort and 96 mice were used in total. Mice were anesthetized with 2% isoflurane prior to airway instillation. Mice were anesthetized with 2% isoflurane prior to airway instillation. Mice in the PBS control group received phosphate-buffered saline (PBS, 50 μL) intratracheally and were then administered PBS (100 μL) intravenously 4 h after instillation. To establish bacterial lung injury, mice were challenged intratracheally with *E. coli* (2 × 10^6 CFU) in a total volume of 50 μL, followed by intravenous PBS (100 μL) at 4 h after instillation. For pharmacological intervention, *E. coli*-challenged mice were treated with LXA4 (7 μg/kg) intravenously in 100 μL at 4 h post-challenge. For receptor antagonism, *E. coli*-challenged mice received LXA4 (7 μg/kg, i.v.) plus WRW4 (1.8 mg/kg), administered intraperitoneally in 200 μL at the same 4 h time point. The dosing regimen and time points were determined based on published literature and preliminary experiments. The bacterial inoculum was prepared freshly for each experiment and the delivered CFU was verified by serial-dilution plating on LB agar. Each mouse was maintained in individual housing throughout the experimental period.

Exclusion criteria were predefined before group allocation and included technical failure of intratracheal instillation, sample loss/contamination, or unexpected death before scheduled endpoints. Animals were monitored at least twice daily for respiratory distress, reduced mobility, ruffled fur, or >15% weight loss. Humane endpoint criteria included severe dyspnea, inability to access food/water, hypothermia, or >20% weight loss, triggering immediate euthanasia. No peri-procedural analgesics were administered, as procedures were performed under brief isoflurane anesthesia and endpoints were short; animals showing unexpected pain/distress would have received rescue analgesia and/or immediate euthanasia according to the approved protocol. No animals were excluded and no animals met humane endpoint criteria before scheduled sample collection.

Investigators performing outcome assessments (histology scoring, ELISA/CFU counting, image quantification) and statistical analysis were blinded to group allocation; treatments were prepared/administered by a separate investigator not involved in readouts. To minimise potential confounders, all groups were maintained under identical housing conditions and followed a standardized experimental protocol. Treatments and subsequent sampling/measurements were performed in an alternating, interleaved group order within the same batch to balance potential order effects. Wherever possible, procedures were conducted by the same operator using consistent equipment settings, and samples were processed in parallel under coded identifiers to reduce batch effects.

Cell Culture and Treatment

Murine alveolar macrophage MH-S cells were cultured in recommended complete medium at 37 °C in a humidified incubator with 5% CO_2. Cells in logarithmic growth phase were seeded into 6-well plates at 5 × 10^6 cells per well. For stimulation, cells were exposed to LPS (1 μg/mL) for 24 h. Where indicated, LXA4 (200 nM) was added 30 min before LPS challenge and maintained during subsequent stimulation. In receptor-blocked experiments, WRW4 (10 μM) was co-administered with LXA4 during the 30 min pretreatment period prior to LPS exposure. Control cells received an equivalent volume of complete medium (2 mL per well) without additional reagents. After 24 h, culture supernatants and cells were collected for downstream analyses. All in vitro assays were performed as at least three independent biological replicates on different days using MH-S cells within a limited passage range to minimize passage-related variability, with technical replicates averaged before statistical analysis when applicable. LPS-stimulated MH-S cells were used as a reductionist macrophage model of Gram-negative inflammatory activation, whereas the *E. coli* mouse model was used to evaluate integrated lung injury and viable bacterial clearance.

Sample Collection

At 24 h and 72 h after *E. coli* instillation, samples were collected from two independent in vivo cohorts. For the BALF/plasma cohort, mice were deeply anesthetized with isoflurane, blood was obtained from the retro-orbital plexus, centrifuged at 4 °C (3000 rpm, 10 min), and plasma was stored at −80 °C until analysis for sample collection. BALF was collected after tracheal exposure by instilling 1 mL of precooled sterile PBS into the airway and gently aspirating the fluid three times to maximize recovery.[29] For the lung-tissue cohort, mice were euthanized at the same time points without prior BALF lavage, and lungs were harvested for histology, ROS measurement, and Western blotting. After completion of sampling, animals were euthanized in accordance with the AVMA Guidelines for the Euthanasia of Animals: mice were first rendered deeply unconscious by isoflurane overdose (≥4–5% in oxygen) until breathing ceased, followed immediately by cervical dislocation performed by trained personnel as a secondary physical method. Death was confirmed by the absence of respiration and heartbeat and lack of reflexes. For histological assessment, lung tissue was fixed in 4% paraformaldehyde for 24 h at room temperature, dehydrated through graded ethanol (70–100%), embedded in paraffin, sectioned, and stained with hematoxylin and eosin (H&E). The remaining lung tissue was snap-frozen in liquid nitrogen and stored at −80 °C for subsequent molecular analyses.

Lung Histology and Injury Scoring

The lung tissues were collected from the model mice, rinsed with pre-cooled PBS, fixed in 4% paraformaldehyde for 24 h, dehydrated, embedded in paraffin, sectioned (4–5 μm), and mounted on slides. For HE staining, sections were deparaffinized, rehydrated, stained with hematoxylin and eosin sequentially (with differentiation and bluing steps), dehydrated again, cleared, and mounted. Finally, sections were observed and imaged under an optical microscope (OLYMPUS, Tokyo, Japan).

Lung injury was scored using the Smith scoring system by two independent, blinded observers. Alveolar congestion, hemorrhage, inflammatory cell infiltration, and alveolar septal thickening/edema were each graded on a 0–4 scale (0, absent; 4, severe), and the sum of all parameters was reported as the total injury score (0–16).[30] For each mouse, 10 randomly selected high-power fields (400×) were assessed and averaged to obtain a representative score. Excellent inter-rater agreement was achieved (intraclass correlation coefficient, ICC = 0.89).

BALF Bacterial Colony Enumeration and Protein Measurement

Bacterial burden in BALF was determined under sterile conditions in a biosafety cabinet. LB agar plates were prepared with sterile glass beads, after which 100 μL of undiluted BALF or a 10-fold dilution was applied to the plate surface and evenly distributed by gentle shaking. Beads were removed, plates were incubated at 37 °C for 24 h, and colonies were counted. Results were expressed as CFU/mL. BALF total protein concentration was measured using a BCA protein assay kit according to the manufacturer's instructions, A standard curve was generated using serially diluted bovine serum albumin standards, absorbance was recorded at 562 nm, and protein concentrations were calculated from the standard curve and expressed as μg/mL.

Cytokine and Lipid Mediator Measurement by ELISA

BALF, plasma, and cell culture supernatants were clarified by centrifugation at 4 °C (3000 rpm, 10 min) to remove cellular debris. Concentrations of IL-1β, TNF-α, IL-6, and IL-10 were quantified using commercial ELISA kits according to the manufacturer's protocols. Absorbance was recorded at 450 nm, and cytokine concentrations were calculated from standard curves. Plasma LXA4, LTB4, LTC4, and PGE2 were quantified using commercial ELISA kits according to the manufacturer's instructions. These lipid mediator measurements were interpreted as supportive pharmacodynamic readouts.

Western Blotting

Lung tissues were homogenized in lysis buffer and centrifuged at 14,000 rpm for 30 min to obtain cleared lysates. Protein concentrations were determined using the BCA assay. Equal amounts of protein (30 μg) were separated by SDS–PAGE and transferred onto PVDF membranes. The membranes were blocked with 5% nonfat milk for 1 h at room temperature and incubated overnight at 4 °C with primary antibody against HO-1 (1:1000). After three washes with TBST, membranes were incubated with HRP-conjugated secondary antibody (1:5000) for 1 h at room temperature. Signals were visualized using enhanced chemiluminescence (ECL). Band intensities were quantified with ImageJ and normalized to β-actin.

RT–qPCR

Total RNA (1 μg) was reverse-transcribed into cDNA using commercial reverse transcription reagents. Quantitative PCR was performed under the following conditions: 95 °C for 10 min, followed by 40 cycles of 95 °C for 15s and 60 °C for 1 min. Relative mRNA levels of STAT1 and STAT3 were calculated using the 2^−ΔΔCt method, with β-actin used as the reference gene. Primer sequences are listed in Table 1.

Measurement of Lung ROS

Fresh lung tissue was minced and mechanically dispersed in cold saline to generate a cell-enriched suspension. Suspensions were adjusted to 1 × 10^7 cells per sample and then incubated with 10 μM DCFH-DA at 37 °C for 20 min. Fluorescence was measured at 488 nm excitation and 525 nm emission wavelengths, and ROS production was expressed as relative fluorescence intensity. Fluorescence-based ROS measurement was interpreted as a supportive oxidative stress readout rather than a species-specific ROS assay.

Immunofluorescence Staining

Following treatment, MH-S cells were washed three times with PBS, fixed in 4% paraformaldehyde for 15 min, and permeabilized with 0.5% Triton X-100 for 20 min. After blocking with 3% bovine serum albumin for 60 min, cells were incubated overnight at 4 °C with primary antibodies against iNOS and CD206 (1:200). Cells were then washed three times and incubated with fluorescently labeled secondary antibodies (1:500) for 1 h at room temperature in the dark. Nuclei were counterstained with DAPI for 5 min, and samples were mounted using an anti-fade medium. Images were acquired by fluorescence microscopy (OLYMPUS, Tokyo, Japan) using identical exposure, gain, and magnification settings within each experiment. Any contrast adjustments were applied uniformly across groups. Signal intensity was quantified using ImageJ under coded conditions, and values from multiple fields were averaged to generate one biological replicate-level value.

Table 1 Primer Information for RT-qPCR in MH-S Cells

Gene Name	Forward Primer	Reverse Primer
STAT1	AATCCACCAACGGAAGTCTGG	AAGAGAGGTGGTCTGAAAGGG
STAT3	AACGACCTGCAGCAATACCA	TCCATGTCAAACGTGAGCGA
β-actin	GTGCTATGTTGCTCTAGACTTC	ATGCCACAGGATTCCATACC

https://doi.org/10.2147/JIR.S597266

Phagocytosis Assay

After the indicated treatments, the medium was replaced with fresh complete medium and GFP-labeled *E. coli* (2.5 × 10^6 per well) was added for 90 min at 37 °C in the dark. Cells were washed three times with PBS to remove extracellular bacteria. Membranes were stained with DiI for 20 min at 37 °C (protected from light), and cell-associated bacterial uptake was assessed by fluorescence microscopy (GFP, green; DiI, red). GFP signal was quantified from coded images using consistent thresholding rules in ImageJ and normalized to cell number or field area as appropriate. This assay reflects cell-associated bacterial uptake; intracellular bacterial killing was not directly measured.

Statistical Analysis

Data were analyzed using GraphPad Prism 8.0 (GraphPad Software, USA) and are presented as mean ± SD. Normality was assessed using the Shapiro–Wilk test, and homogeneity of variances was assessed using Levene's test. For in vivo endpoints measured at 24 h and 72 h, treatment group, time, and treatment × time interaction were evaluated using two-way ANOVA followed by Tukey's multiple-comparisons test when assumptions were met. When assumptions were violated, analyses were performed separately at each time point using Kruskal–Wallis tests followed by Dunn's multiple-comparisons test. Single-timepoint in vitro assays were analyzed using one-way ANOVA followed by Tukey's post hoc test or Kruskal–Wallis testing with Dunn's post hoc test when appropriate. Lung injury score, BALF protein, BALF CFU, and BALF cytokines were defined as key injury/inflammation-related readouts; plasma lipid mediators, ROS fluorescence, HO-1 expression, and in vitro macrophage assays were interpreted as supportive mechanistic readouts. A p value < 0.05 was considered statistically significant.

Results

LXA4 Attenuates Macroscopic and Histopathological Lung Injury After E. coli Challenge

We evaluated lung injury in mice at the early stage (24 h) and late stage (72 h) after model establishment.[31,32] PBS-treated mice showed uniformly pink lungs without visible lesions, whereas ARDS mice developed marked hyperemia with diffuse congestion and petechial hemorrhages (Figure 1A). Compared with the ARDS model group, LXA4 substantially improved gross appearance, and these macroscopic benefits were weakened by the ALX/FPR2 antagonist WRW4. Consistently, ARDS induction elevated the lung wet weight-to-body weight ratio at both time points, reflecting the development of pulmonary edema; LXA4 significantly reduced this ratio, whereas LXA4 + WRW4 partially attenuated this effect, with a more evident reversal at 72 h (Figure 1B). Histologically, PBS lungs preserved intact alveolar architecture, but ARDS lungs exhibited prominent inflammatory infiltration, septal thickening/edema, and focal structural disruption at 24 h that persisted at 72 h with elevated injury scores (Figure 1C and D). LXA4 mitigated these pathological changes and lowered histological scores, whereas LXA4 + WRW4 diminished LXA4-mediated protection, supporting pharmacological involvement of ALX/FPR2 signaling (Figure 1C and D).

LXA4 Dampens Airway Inflammation, Preserves Barrier Function, and Promotes Bacterial Clearance in BALF

Compared with PBS controls, ARDS mice displayed markedly elevated BALF IL-6, IL-1β, and TNF-α at 24 h and 72 h, indicating robust airway inflammation. LXA4 significantly reduced these cytokines, whereas LXA4 + WRW4 largely abolished this suppression (Figure 2A). In parallel, total BALF protein rose substantially in ARDS mice at both time points, consistent with alveolar–capillary barrier disruption; LXA4 lowered BALF protein levels, and LXA4 + WRW4 showed a partial but non-significant reversal of this reduction (Figure 2B). BALF CFU counts were negligible in PBS mice but high after *E. coli* challenge, with partial decline by 72 h; LXA4 further reduced CFUs at both time points, while LXA4 + WRW4 shifted bacterial counts back toward ARDS levels, indicating that LXA4-enhanced bacterial handling is at least partly ALX/FPR2-associated (Figure 2B).

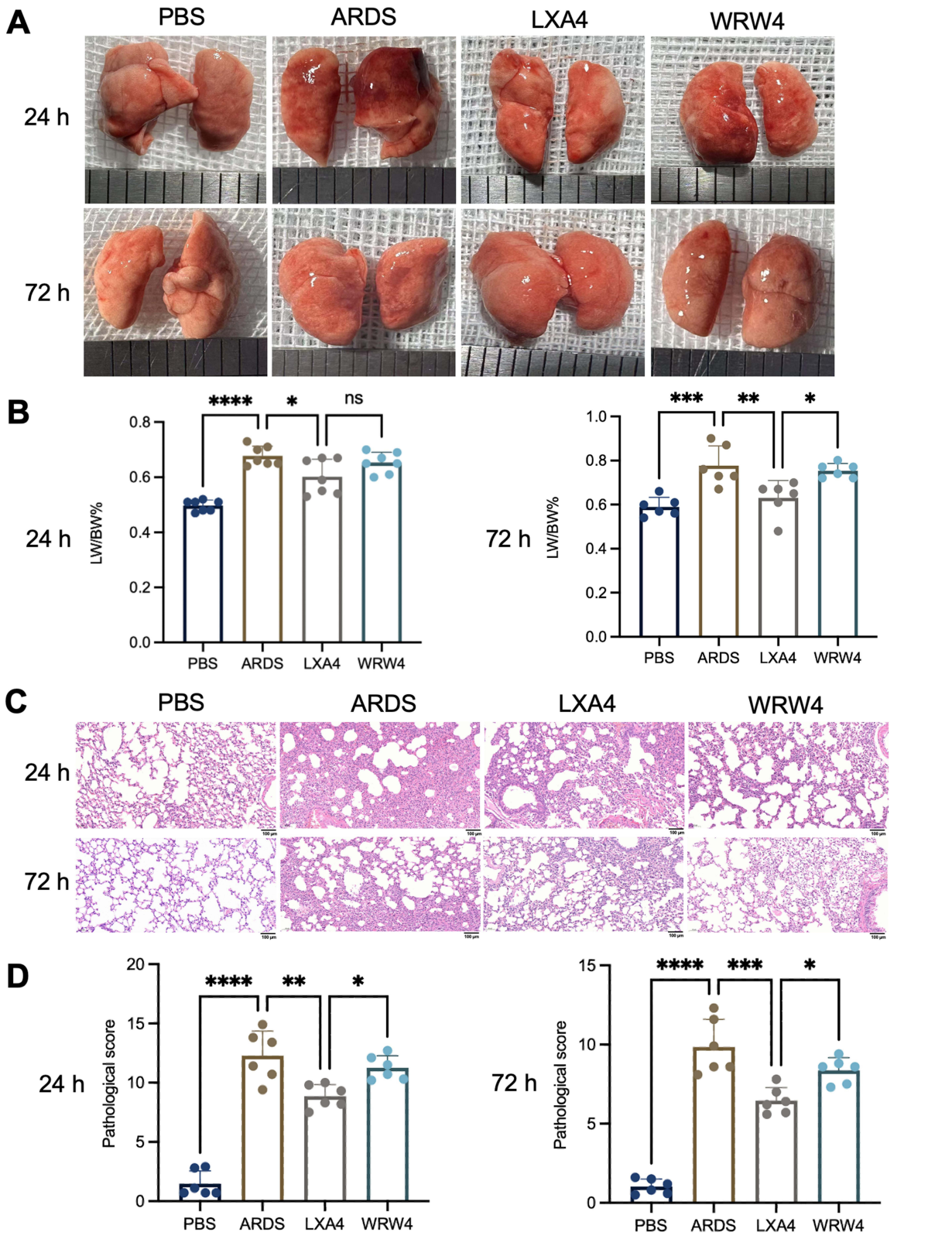

Figure 1 LXA4 attenuates macroscopic and histopathological lung injury after *E. coli* Challenge. (**A**) General lung appearance following *E. coli* challenge and LXA4 treatment. (**B**) Lung wet weight-to-body weight ratio. (**C**) H&E staining of mouse lung tissue at 24 h and 72 h post *E. coli* challenge and LXA4 treatment (100× magnification, scale bar = 100 μm). (**D**) Histologic lung injury quantified via Smith scoring system. PBS group: intratracheal PBS followed by intravenous PBS; ARDS group: intratracheal *E. coli* followed by intravenous PBS; LXA4 group: intratracheal *E. coli* followed by intravenous 7 μg/kg LXA4; LXA4 + WRW4 group: intratracheal *E. coli* followed by intravenous 7 μg/kg LXA4 plus intraperitoneal 1.8 mg/kg WRW4. Data are presented as mean ± SD with individual data points shown; n=6 mice per group per time point; *p < 0.05, **p < 0.01, ***p < 0.001, ****p < 0.0001; ns, not significant.

https://doi.org/10.2147/JIR.S597266

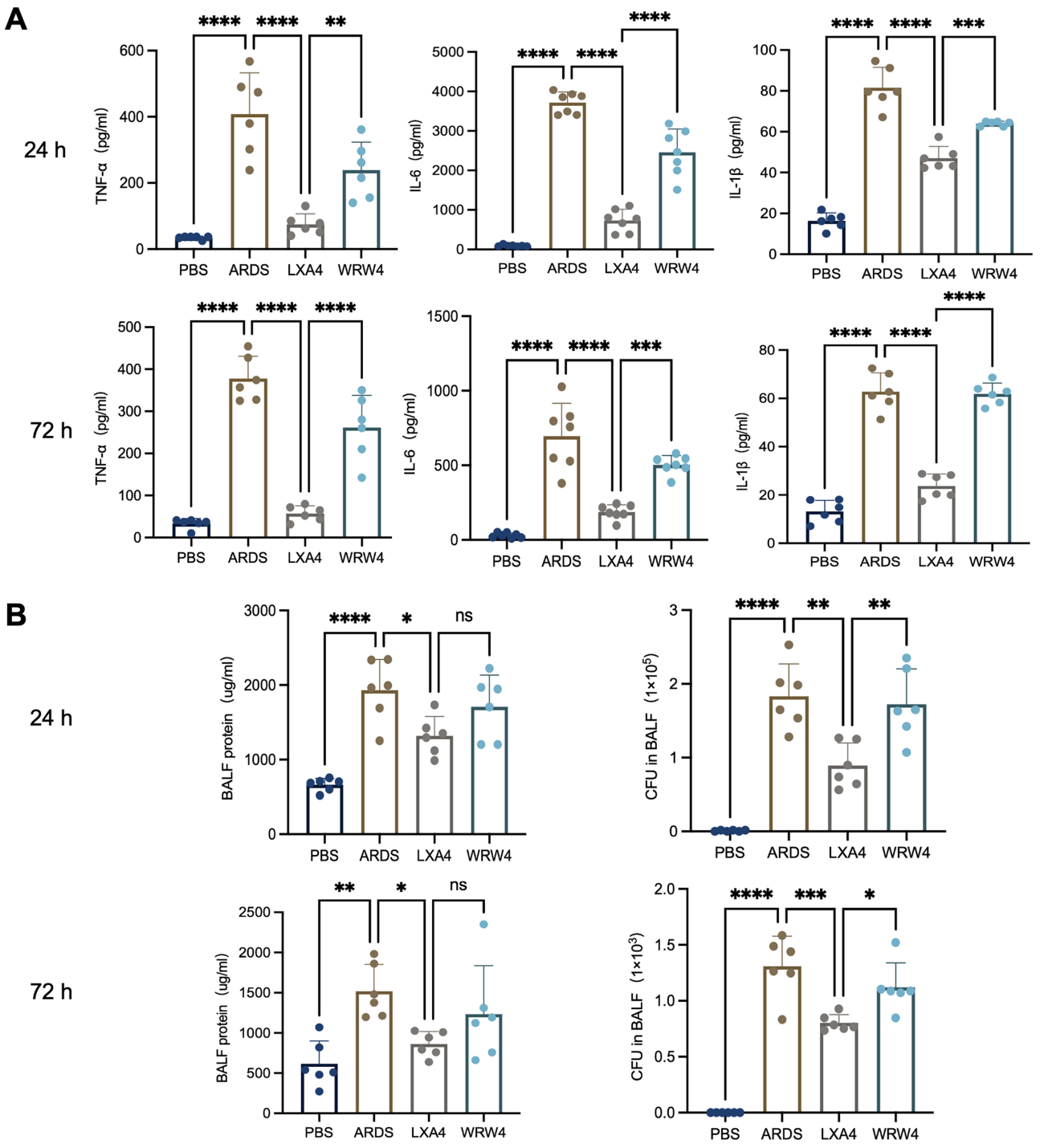

Figure 2 LXA4 suppresses BALF cytokines, reduces barrier leakage, and enhances bacterial handling in BALF in an ALX/FPR2-dependent manner. (**A**) TNF-α, IL-6 and IL-1β levels in mouse BALF at 24 h and 72 h post *E. coli* challenge and LXA4 treatment by ELISA. (**B**) Protein concentration and bacterial colony counts in mouse BALF. Data are presented as mean ± SD with individual data points shown; n=6 mice per group per time point; *$p < 0.05$, **$p < 0.01$, ***$p < 0.001$, ****$p < 0.0001$; ns, not significant.

LXA4 Reprograms Systemic Lipid Mediators and Mitigates Oxidative Stress in Lung Tissue

Relative to PBS controls, ARDS mice displayed elevated plasma LTB4 and LTC4, and PGE2 increased prominently by 72 h, consistent with a systemic pro-inflammatory lipid signature. Exogenous LXA4 administration increased circulating LXA4 levels while suppressing LTB4, LTC4, and PGE2. Co-treatment with WRW4 partially counteracted these LXA4-

associated changes in plasma lipid mediator readouts, although the magnitude of reversal differed among individual mediators and time points (Figure 3A). ROS and HO-1 levels in lung tissue were examined at 24 h and 72 h. ARDS challenge increased lung ROS and was accompanied by elevated HO-1 expression compared with PBS controls, possibly reflecting an endogenous compensatory antioxidant response. LXA4 reduced ROS and further increased HO-1 expression, whereas LXA4 + WRW4 partially attenuated the LXA4-associated HO-1 increase; its reversal of ROS reduction was less pronounced (Figure 3B).

LXA4 Promotes an M2-Like Macrophage Marker Profile via ALX/FPR2

To further investigate the role of LXA4 in macrophage responses, MH-S cells were employed as an in vitro alveolar macrophage model. LPS stimulation significantly upregulated STAT1 and STAT3 mRNA expression. LXA4 reduced STAT1 expression and further enhanced STAT3 expression relative to LPS alone, a pattern consistent with a shift away from a strongly pro-inflammatory state. WRW4 significantly attenuated the LXA4-associated increase in STAT3, whereas reversal of STAT1 reduction was less pronounced (Figure 4A). Immunofluorescence showed that LXA4 decreased iNOS and increased CD206 signals relative to LPS alone; WRW4 significantly attenuated the CD206 increase, whereas its

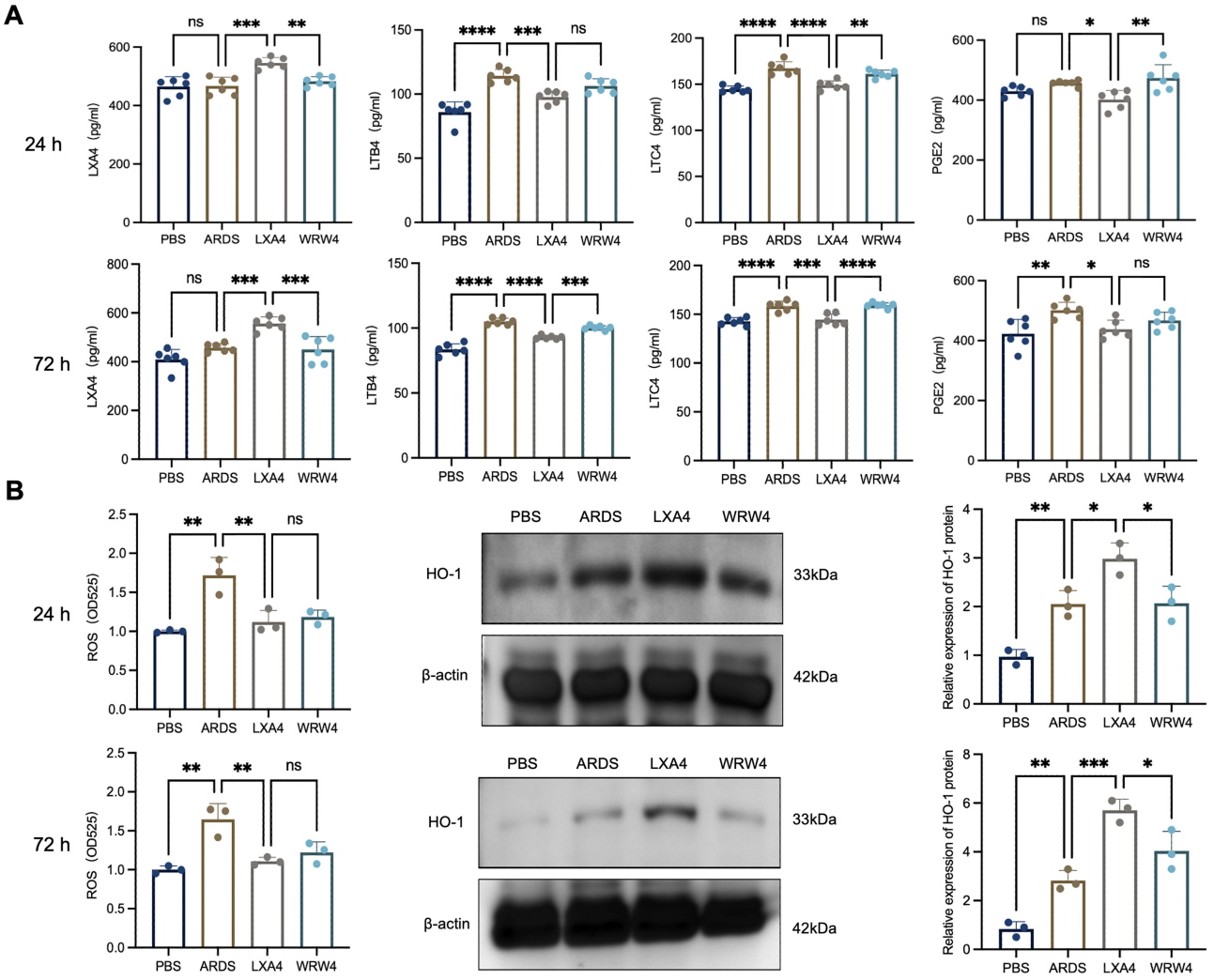

Figure 3 LXA4 remodels circulating lipid mediators readouts and alleviates pulmonary oxidative stress through ALX/FPR2 signaling. (**A**) Plasma levels of LXA4, LTB4, LTC4, and PGE2 in mice at 24 h and 72 h post *E. coli* challenge and LXA4 treatment by ELISA. (**B**) ROS levels and HO-1 protein expression in mouse lung tissue at 24 h and 72 h post *E. coli* challenge and LXA4 treatment. Data are presented as mean ± SD with individual data points shown; n=6 mice per group per time point; for ROS and Western blot analyses, n=3 independent lung-tissue samples per group per time point. *$p < 0.05$, **$p < 0.01$, ***$p < 0.001$, ****$p < 0.0001$; ns, not significant.

https://doi.org/10.2147/JIR.S597266

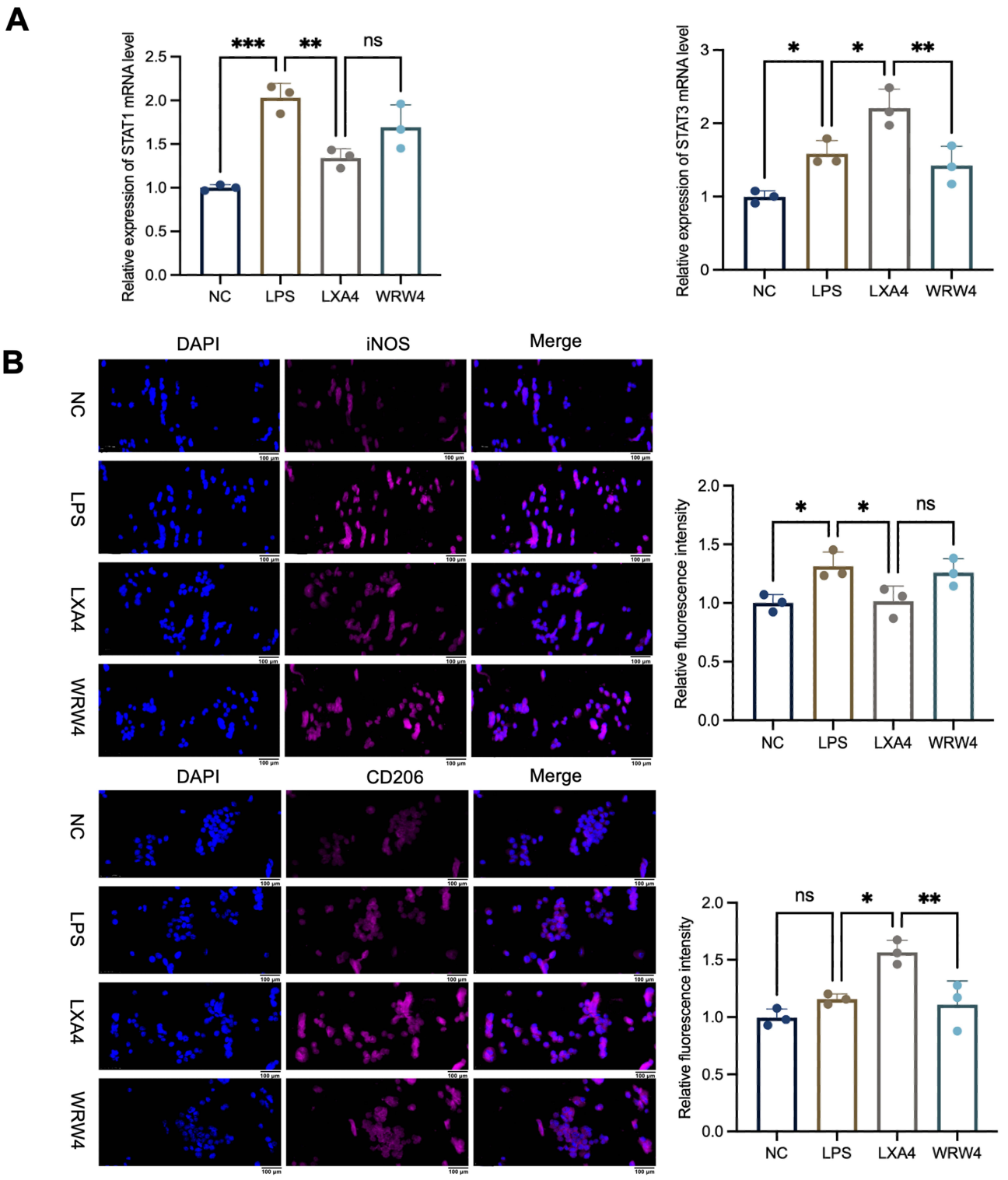

Figure 4 LXA4 promotes an M2-like macrophage marker profile in MH-S cells via ALX/FPR2–dependent macrophage reprogramming. (**A**) RT-qPCR analysis of STAT1 and STAT3 mRNA. (**B**) immunofluorescence for iNOS and CD206 proteins in MH-S cells post LPS and LXA4 treatment. NC group: vehicle control; LPS group: 1 μg/mL LPS; LXA4 group: 200 nM LXA4 plus LPS; LXA4 + WRW4 group: 200 nM LXA4 plus LPS plus 10 μM WRW4. Data are presented as mean ± SD with individual data points shown; n=3 independent biological replicates. *$p < 0.05$, **$p < 0.01$, ***$p < 0.001$, ****$p < 0.0001$; ns, not significant.

https://doi.org/10.2147/JIR.S597266

effect on iNOS reversal was weaker (Figure 4B). These data support macrophage phenotypic modulation but do not constitute comprehensive macrophage state mapping.

LXA4 Rebalances Macrophage Cytokine Secretion and Enhances Phagocytic Capacity Through ALX/FPR2

In MH-S supernatants, LPS stimulation markedly increased IL-1β and TNF-α, consistent with a pro-inflammatory secretory phenotype. LXA4 pretreatment significantly reduced IL-1β and TNF-α and restored IL-10 levels, indicating a shift toward a more pro-resolving cytokine profile. WRW4 significantly attenuated the LXA4-mediated reduction in TNF-α, whereas its effects on IL-1β and IL-10 were less pronounced (Figure 5A). Because macrophage-mediated bacterial clearance is critical during bacterial ARDS, we next evaluated cell-associated bacterial uptake using GFP-labeled *E. coli*. Compared with LPS alone, LXA4-treated cells exhibited increased cell-associated GFP-*E. coli* signal after washing, indicating enhanced bacterial uptake. WRW4 significantly diminished this increase, suggesting that LXA4 augments macrophage bacterial handling through an ALX/FPR2-dependent mechanism (Figure 5B).

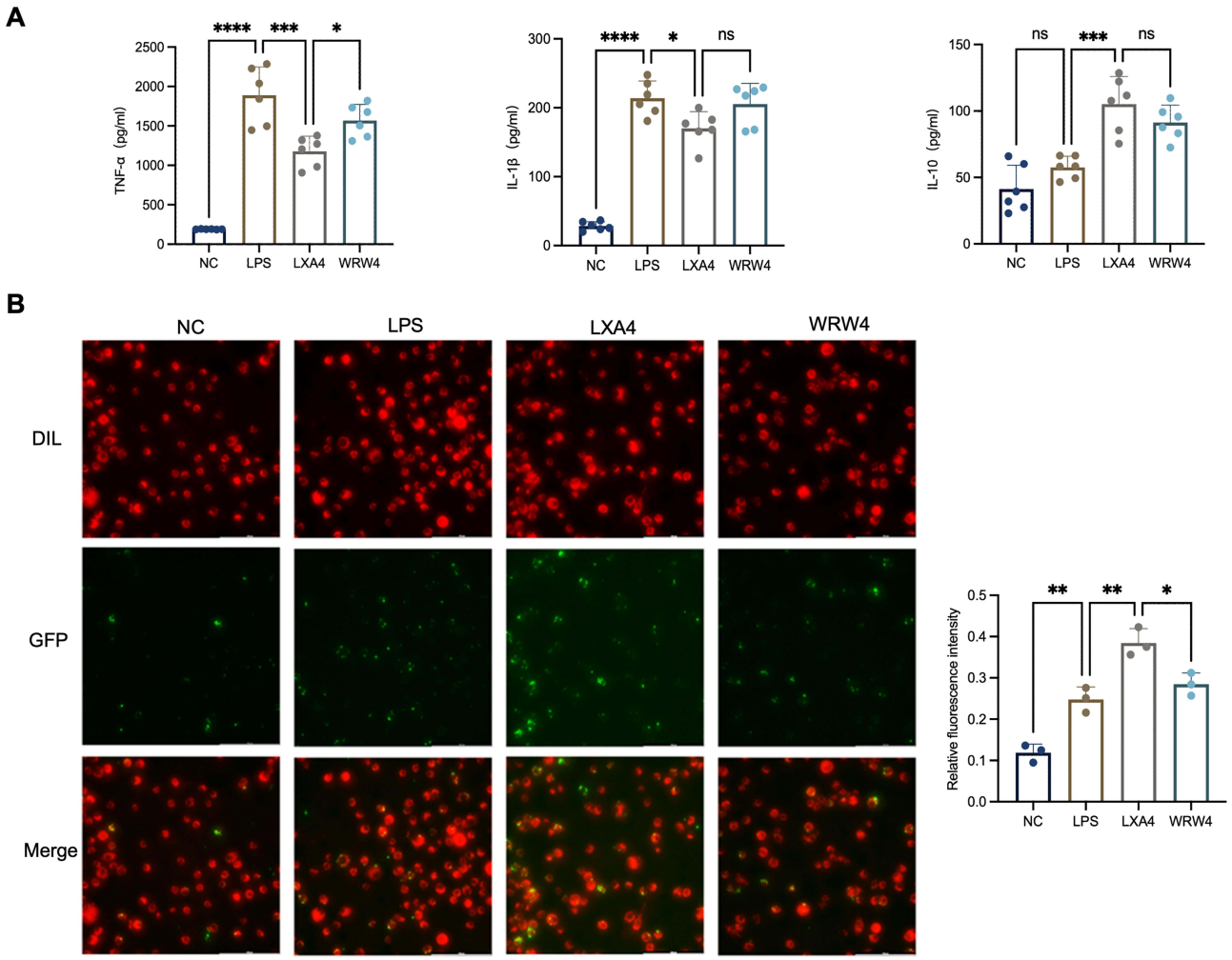

Figure 5 LXA4 rebalances macrophage cytokine secretion and enhances cell-associated bacterial uptake through ALX/FPR2-dependent macrophage reprogramming. (**A**) IL-1β, TNF-α, and IL-10 levels in MH-S cell supernatants after LPS and LXA4 treatment by ELISA. (**B**) Cell-associated uptake of GFP-*E. coli* by MH-S cells after LPS and LXA4 treatment. Dil (red) stains cell membranes; GFP-*E. coli* appears green. Images were acquired and processed using identical settings within each experiment. Data are presented as mean ± SD with individual data points shown; n=3–6 independent biological replicates; *$p < 0.05$, **$p < 0.01$, ***$p < 0.001$, ****$p < 0.0001$; ns, not significant.

https://doi.org/10.2147/JIR.S597266

Discussion

ALI/ARDS represents a frequent and severe complication, typically manifested by alveolar flooding and extensive recruitment of inflammatory cells.[2,33] Its onset and progression are driven by multifactorial mechanisms in which uncontrolled inflammation, disruption of endothelial integrity, oxidative stress, and cell death interact in a self-amplifying manner.[34] Despite advances in supportive care, current therapeutic options remain insufficient to effectively interrupt disease escalation.[35] We employed an in vivo *E. coli*–induced murine ARDS-like model and an in vitro LPS-stimulated MH-S macrophage system to evaluate whether LXA4 attenuates bacterial lung injury via ALX/FPR2 signaling. LXA4 reduced pulmonary edema, histologic injury, BALF cytokines, barrier leakage, bacterial burden, and modulated systemic lipid mediators. In vitro, LXA4 promoted an M2-like macrophage phenotype and enhanced cell-associated bacterial uptake. These effects were partially reversed by the ALX/FPR2 antagonist WRW4, supporting receptor involvement. Overall, our findings suggest LXA4 exerts protective effects in infection-driven ARDS-like injury via ALX/FPR2-associated pro-resolving mechanisms. Experimental design and outcomes are summarized in Figure 6.

A central pathological feature of ARDS is increased alveolar–capillary permeability leading to protein-rich edema and impaired gas exchange.[2,36] In our model, the convergence of a reduced lung wet weight/body weight ratio, lower BALF protein, and improved histological injury scores after LXA4 treatment indicates a coordinated effect on vascular–epithelial barrier integrity rather than isolated cytokine suppression. These findings align with the concept that successful ARDS interventions must interrupt feed-forward loops connecting leukocyte recruitment, endothelial activation, and epithelial injury.[37] Mechanistically, LXA4 has been shown to support epithelial repair programs and alveolar fluid handling (including ENaC/Na, K-ATPase-linked pathways), providing a biologically plausible basis for the anti-edematous phenotype observed here.[38,39] Importantly, WRW4 weakened the macroscopic, edema, and histologic improvements, arguing that barrier protection is not simply a nonspecific lipid effect but instead reflects ALX/FPR2-dependent signaling within the injured lung microenvironment.[21,40]

The airway inflammatory response in bacterial ARDS is often dominated by IL-6, IL-1β, and TNF-α, which amplify neutrophil trafficking, endothelial leak, and epithelial dysfunction.[2,41] LXA4 reduced all three cytokines in BALF at both 24 h and 72 h, suggesting that LXA4 does not merely delay inflammation but promotes a more rapid inflammatory

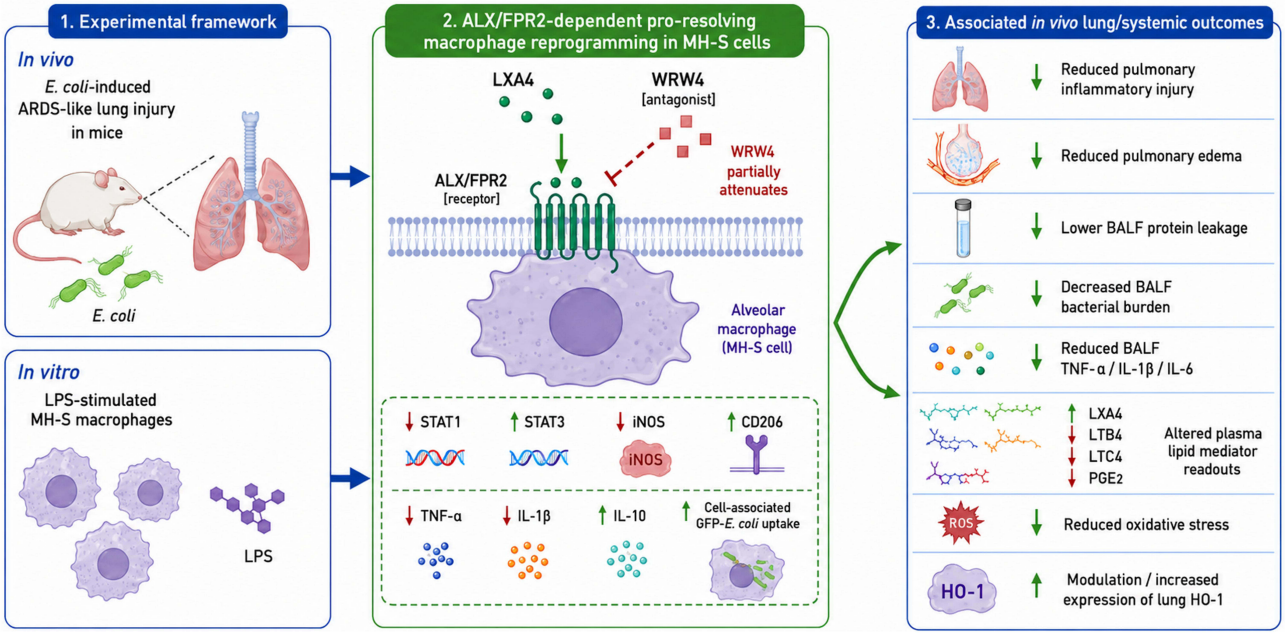

Figure 6 Proposed model for LXA4-mediated attenuation of *E. coli*-induced ARDS-like lung injury. LXA4 treatment was associated with reduced pulmonary inflammatory injury, lower BALF protein leakage, decreased BALF bacterial burden, altered plasma lipid mediator readouts, reduced oxidative stress, and modulation of lung HO-1 expression. In MH-S macrophages, LXA4 promoted a pro-resolving marker profile, including reduced STAT1/iNOS and increased STAT3/CD206/IL-10 signals, and enhanced cell-associated GFP-*E. coli* uptake. WRW4 partially attenuated these effects, supporting pharmacological involvement of ALX/FPR2 signaling. Cell-specific ALX/FPR2 mechanisms remain to be validated.

downshift across early and late phases of injury. This temporal persistence is relevant because late-stage ARDS is frequently sustained by unresolved inflammation and defective repair.[42] Our observation that WRW4 largely abolished cytokine suppression supports a model in which ALX/FPR2 functions as a molecular switch toward resolution, consistent with broader pro-resolving mediator biology.[21,40] Taken together, the cytokine and barrier findings suggest that LXA4 acts upstream of tissue-level injury amplification—reducing inflammatory tone while simultaneously stabilizing the interface where edema forms.[42,43]

Beyond protein/cytokine readouts, the plasma lipid mediator profile provides an integrated view of systemic inflammatory bias. LXA4 increased circulating LXA4 while suppressing LTB4, LTC4, and PGE2, all of which can promote leukocyte recruitment, vascular permeability, and immune dysregulation depending on context.[44–46] The LTB4–BLT axis is a well-established driver of neutrophil chemotaxis and amplification of acute inflammation, while cysteinyl leukotrienes contribute to microvascular leak and bronchovesicular responses.[47,48] In parallel, PGE2 exerts context-dependent immunoregulatory effects that may impair selected antimicrobial functions when excessive or prolonged. In this setting, LXA4-associated suppression of these mediators is compatible with a shift from propagation toward resolution,[49] although these ELISA-based measurements should be interpreted as supportive pharmacodynamic readouts rather than definitive lipidomic profiling.[50]

A major translational challenge in ARDS is achieving inflammation control without compromising pathogen clearance.[51] Our data address this concern: LXA4 reduced BALF CFU at both time points and enhanced cell-associated GFP-*E. coli* uptake by MH-S macrophages in vitro, while WRW4 blunted these benefits. This pattern supports an emerging paradigm in which pro-resolving mediators can limit collateral inflammatory damage and preserve (or enhance) host defense.[24,52] Consistent with this, ALX/FPR2 signaling has been implicated in effective host responses during bacterial lung infection; pharmacologic disruption of the lipoxin/resolvin receptor axis worsens outcomes in pneumococcal pneumonia-associated lung injury, underscoring the receptor's role in coordinating resolution with antimicrobial competence.[24,53] In our study, the coupling of reduced pro-inflammatory cytokines with improved bacterial handling argues that LXA4 promotes a functional macrophage state optimized for clearance with restrained tissue-destructive signaling, rather than immunosuppression. However, intracellular bacterial killing was not directly measured and requires further validation.

Our macrophage data provide mechanistic support for a pro-resolving phenotype. LXA4 decreased iNOS and increased CD206, reduced IL-1β/TNF-α while restoring IL-10, and differentially regulated STAT1 and STAT3 transcripts. STAT1 is commonly associated with inflammatory macrophage activation, whereas STAT3 can integrate anti-inflammatory and tissue-protective signals depending on context.[54–56] Thus, the combined marker and functional findings are consistent with an M2-like, pro-resolving shift. Nevertheless, macrophage polarization in ARDS is more complex than a binary M1/M2 model, and these markers do not exhaustively define macrophage states.

Oxidative stress is another amplifier of epithelial and endothelial injury in ARDS, contributing to barrier failure, cell death, and dysregulated repair.[27,57–59] In the present study, *E. coli*-induced ARDS-like injury increased lung ROS and was accompanied by elevated HO-1 expression, likely reflecting an endogenous but insufficient compensatory antioxidant response. LXA4 reduced oxidative burden while further enhancing HO-1 expression, whereas WRW4 partially attenuated the LXA4-associated HO-1 increase. The reversal of ROS reduction by WRW4 was less pronounced.[40,60] These findings suggest that LXA4-mediated lung protection is associated with coordinated attenuation of oxidative stress and augmentation of adaptive antioxidant signaling.

The novelty of this study lies not merely in confirming the anti-inflammatory effects of LXA4, but in integrating multiple dimensions—including bacterial burden, systemic lipid mediator remodeling, macrophage phenotype and function, oxidative stress, and both in vivo and in vitro ALX/FPR2 antagonism—within a post-injury *E. coli* live-bacteria ARDS-like model. Unlike most previous studies that employed sterile LPS-induced ALI models, the present study administered LXA4 therapeutically at 4 h post-injury, better reflecting an early treatment window in bacterial pneumonia-induced ARDS. Importantly, LXA4 attenuated lung injury, inflammation, and oxidative stress while reducing, rather than increasing, BALF bacterial burden, addressing a key translational concern regarding anti-inflammatory therapy and host defense.[61,62] Collectively, this study provides more comprehensive and rigorous mechanistic evidence for LXA4/ALX-FPR2-mediated pro-resolving effects in infection-associated ARDS than prior investigations.[61,63,64]

Several limitations should be considered. First, the *E. coli* model captures selected features of infection-driven ARDS, including edema, cytokine elevation, barrier disruption, bacterial burden, and histological injury, but it does not encompass viral pneumonia, polymicrobial infection, aspiration, ventilator-induced injury, comorbidities, or interactions with supportive care.[21,38] Second, only male mice were used, and sex-dependent effects of LXA4/ALX-FPR2 signaling remain to be tested. Third, WRW4 provides pharmacological evidence for ALX/FPR2 involvement but cannot identify the dominant ALX/FPR2-expressing effector cell type, such as macrophages, epithelium, or endothelium.[43] Fourth, macrophage polarization was assessed using selected markers and functional assays rather than flow cytometry or single-cell profiling.[65] Fifth, the dosing regimen involved a single early post-injury LXA4 administration and does not define optimal timing, repeated dosing, or long-term outcomes.[66] Finally, no formal a priori power calculation was performed, and smaller treatment-by-time interactions may be underpowered.

Future studies should validate these findings in sex-balanced cohorts, additional bacterial and viral ARDS models, primary human macrophages, and cell-specific ALX/FPR2 genetic systems. Complementary flow cytometric phagocytosis, intracellular killing, lung mechanics, oxygenation, survival, and longer-term repair endpoints would further clarify translational potential.

Conclusion

This study demonstrates that LXA4 confers ALX/FPR2-dependent protection against *E. coli*-induced ARDS-like lung injury in mice by integrating barrier stabilization, lipid mediator rebalancing, oxidative stress modulation, and M2-like macrophage phenotypic reprogramming, while preserving bacterial clearance. These effects were attenuated by WRW4. The findings support ALX/FPR2-targeted pro-resolving therapy as a rational adjunct strategy for infection-driven lung injury. Further studies are required to define cell-specific mechanisms, sex-dependent differences, optimal dosing, and efficacy in more clinically representative models.

Data Sharing Statement

The data presented in this study are available on request from the corresponding author.

Ethics Statement

Animals were purchased from Chengdu Dashuo Experimental Animal Co., Ltd. (SCXK(Chuan) 2020-0030). The animal study protocol was approved by the Ethics Committee of Sichuan Provincial People's Hospital (2025-426 and date of approval 24 June 2025) and conducted in accordance with the European Community guidelines (Directive 2010/63/EU of the European Parliament and of the Council). This study strictly adheres to the relevant provisions of the ARRIVE Guidelines.

Author Contributions

Meng Xu: Investigation, Validation, Formal analysis, Writing - Original Draft, Writing - Review & Editing. Bingxue Zhang: Investigation, Validation, Formal analysis, Writing - Original Draft, Writing - Review & Editing. Yanling Deng: Formal analysis, Validation, Data curation, Writing - Review & Editing. Donghui Li: Formal analysis, Validation, Methodology, Writing - Review & Editing. Jun Shen: Data curation, Methodology, Writing - Review & Editing. Chun Pan: Conceptualization, Supervision, Project administration, Funding acquisition, Writing - Review & Editing. Hongli He: Conceptualization, Supervision, Project administration, Funding acquisition, Writing - Review & Editing. All authors contributed to the study conception, design, data acquisition, analysis, interpretation, drafting, or critical revision of the manuscript. All authors gave final approval of the version to be published; have agreed on the journal to which the article has been submitted; and agree to be accountable for all aspects of the work.

Funding

This study was partially supported by the National Natural Science Foundation of China (no. 81700073), the Foundation of the General Office of the National Health Commission (ZDYN-2024-A-025), the Key Research and Development Project of Science and Technology of Sichuan Province (2022YFS0605), and the Chengdu Science and Technology Bureau (2024-YF05-01184-SN).

Disclosure

The authors report no conflicts of interest in this work.

References

1. Grotberg JC, Reynolds D, Kraft BD. Management of severe acute respiratory distress syndrome: a primer. *Crit Care*. 2023;27(1):289. doi:10.1186/s13054-023-04572-w
2. Bos LDJ, Ware LB. Acute respiratory distress syndrome: causes, pathophysiology, and phenotypes. *Lancet*. 2022;400(10358):1145–1156. doi:10.1016/S0140-6736(22)01485-4
3. Aschner Y, Correll KA, Beke KM, et al. PTPalpha promotes fibroproliferative responses after acute lung injury. *Am J Physiol Lung Cell Mol Physiol*. 2022;323(1):L69–L83. doi:10.1152/ajplung.00436.2021
4. Turgeon J, Venkatamaran V, Englesakis M, Fan E. Long-term outcomes of patients supported with extracorporeal membrane oxygenation for acute respiratory distress syndrome: a systematic review and meta-analysis. *Intensive Care Med*. 2024;50(3):350–370. doi:10.1007/s00134-023-07301-7
5. Wick KD, Ware LB, Matthay MA. Acute respiratory distress syndrome. *BMJ*. 2024;387e076612. doi:10.1136/bmj-2023-076612
6. Xie R, Tan D, Liu B, et al. Acute respiratory distress syndrome (ARDS): from mechanistic insights to therapeutic strategies. *MedComm*. 2025;6(2):e70074. doi:10.1002/mco2.70074
7. Ye Y, Yang Q, Wei J, et al. RvD1 improves resident alveolar macrophage self-renewal via the ALX/MAPK14/S100A8/A9 pathway in acute respiratory distress syndrome. *J Adv Res*. 2025;67:289–299. doi:10.1016/j.jare.2024.01.017
8. Chen X, Tang J, Shuai W, Meng J, Feng J, Han Z. Macrophage polarization and its role in the pathogenesis of acute lung injury/acute respiratory distress syndrome. *Inflamm Res*. 2020;69(9):883–895. doi:10.1007/s00011-020-01378-2
9. Liu C, Xiao K, Xie L. Advances in the regulation of macrophage polarization by mesenchymal stem cells and implications for ALI/ARDS treatment. *Front Immunol*. 2022;13:928134. doi:10.3389/fimmu.2022.928134
10. Zhang S, Liu Y, Zhang XL, Sun Y, Lu ZH. ANKRD22 aggravates sepsis-induced ARDS and promotes pulmonary M1 macrophage polarization. *J Transl Autoimmun*. 2024;8:100228. doi:10.1016/j.jtauto.2023.100228
11. Yin Z, Song R, Yu T, Fu Y, Ding Y, Nie H. Natural compounds regulate macrophage polarization and alleviate inflammation against ALI/ARDS. *Biomolecules*. 2025;15(2):192. doi:10.3390/biom15020192
12. Xu Y, Zhang C, Cai D, Zhu R, Cao Y. Exosomal miR-155-5p drives widespread macrophage M1 polarization in hypervirulent Klebsiella pneumoniae-induced acute lung injury via the MSK1/p38-MAPK axis. *Cell Mol Biol Lett*. 2023;28(1):92. doi:10.1186/s11658-023-00505-1
13. Wang L, Wang J, Han L, Chen T. Palmatine attenuated lipopolysaccharide-induced acute lung injury by inhibiting M1 phenotype macrophage polarization via NAMPT/TLR2/CCR1 signaling. *J Agric Food Chem*. 2024. doi:10.1021/acs.jafc.3c05597
14. Yang J, Huang X, Yu Q, et al. Extracellular vesicles derived from M2-like macrophages alleviate acute lung injury in a miR-709-mediated manner. *J Extracell Vesicles*. 2024;13(4):e12437. doi:10.1002/jev2.12437
15. Wang X, Zhao H, Lin W, et al. Panax notoginseng saponins ameliorate LPS-induced acute lung injury by promoting STAT6-mediated M2-like macrophage polarization. *Phytomedicine*. 2025;139:156513. doi:10.1016/j.phymed.2025.156513
16. Wang Z, Wang Z. The role of macrophages polarization in sepsis-induced acute lung injury. *Front Immunol*. 2023;14:1209438. doi:10.3389/fimmu.2023.1209438
17. Wang M, Wu D, Liao X, et al. CPT1A-IL-10-mediated macrophage metabolic and phenotypic alterations ameliorate acute lung injury. *Clin Transl Med*. 2024;14(8):e1785. doi:10.1002/ctm2.1785
18. Mei HX, Ye Y, Xu HR, et al. LXA4 inhibits lipopolysaccharide-induced inflammatory cell accumulation by resident macrophages in mice. *J Inflamm Res*. 2021;14:1375–1385. doi:10.2147/JIR.S301292
19. Ba F, Zhou X, Zhang Y, et al. Lipoxin A4 ameliorates alveolar fluid clearance disturbance in lipopolysaccharide-induced lung injury via aquaporin 5 and MAPK signaling pathway. *J Thorac Dis*. 2019;11(8):3599–3608. doi:10.21037/jtd.2019.08.86
20. Cao E, Xu J, Gong Y, et al. Effect of the lipoxin receptor agonist BML-111 on cigarette smoke extract-induced macrophage polarization and inflammation in RAW264.7 cells. *Int J Chron Obstruct Pulmon Dis*. 2023;18:919–932. doi:10.2147/COPD.S395569
21. Li X, Xu H, Liu K, Shi M, Zeng X, Liu X. LXA4 alleviates inflammation and ferroptosis in cigarette smoke induced chronic obstructive pulmonary disease via the ALX/FPR2 receptor. *Int Immunopharmacol*. 2025;151:114322. doi:10.1016/j.intimp.2025.114322
22. Pereira ABM, Gontijo BA, Tanaka S, et al. Aspirin-triggered RvD1 (AT-RvD1) modulates epithelial-mesenchymal transition on bronchial epithelial cells stimulated with cigarette smoke extract. *Prostaglandins Other Lipid Mediat*. 2025;177:106968. doi:10.1016/j.prostaglandins.2025.106968
23. Perretti M, Dalli J. Resolution pharmacology: focus on pro-resolving annexin A1 and lipid mediators for therapeutic innovation in inflammation. *Annu Rev Pharmacol Toxicol*. 2023;63:449–469. doi:10.1146/annurev-pharmtox-051821-042743
24. Siegel ER, Croze RH, Fang X, Matthay MA, Gotts JE. Inhibition of the lipoxin A4 and resolvin D1 receptor impairs host response to acute lung injury caused by pneumococcal pneumonia in mice. *Am J Physiol Lung Cell Mol Physiol*. 2021;320(6):L1085–L1092. doi:10.1152/ajplung.00046.2021
25. Chi J, Cheng J, Wang S, Li C, Chen M. Promising anti-inflammatory tools: biomedical efficacy of lipoxins and their synthetic pathways. *Int J Mol Sci*. 2023;24(17):13282. doi:10.3390/ijms241713282
26. Jerkic M, Gagnon S, Rabani R, et al. Human umbilical cord mesenchymal stromal cells attenuate systemic sepsis in part by enhancing peritoneal macrophage bacterial killing via heme oxygenase-1 induction in rats. *Anesthesiology*. 2020;132(1):140–154. doi:10.1097/ALN.0000000000003018
27. Wang F, Ge R, Cai Y, et al. Oxidative stress in ARDS: mechanisms and therapeutic potential. *Front Pharmacol*. 2025;16:1603287. doi:10.3389/fphar.2025.1603287
28. Yue L, Yan Y. Metabolic regulation in acute respiratory distress syndrome: implications for inflammation and oxidative stress. *Int J Chron Obstruct Pulmon Dis*. 2025;20:373–388. doi:10.2147/COPD.S491687
29. Li J, Lu K, Sun F, et al. Panaxydol attenuates ferroptosis against LPS-induced acute lung injury in mice by Keap1-Nrf2/HO-1 pathway. *J Transl Med*. 2021;19(1):96. doi:10.1186/s12967-021-02745-1

30. Yu J, Shi J, Wang D, et al. Heme oxygenase-1/carbon monoxide-regulated mitochondrial dynamic equilibrium contributes to the attenuation of endotoxin-induced acute lung injury in rats and in lipopolysaccharide-activated macrophages. *Anesthesiology*. 2016;125(6):1190–1201. doi:10.1097/ALN.0000000000001333
31. Domscheit H, Hegeman MA, Carvalho N, Spieth PM. Molecular dynamics of lipopolysaccharide-induced lung injury in rodents. *Front Physiol*. 2020;11:36. doi:10.3389/fphys.2020.00036
32. Asti C, Ruggieri V, Porzio S, Chiusaroli R, Melillo G, Caselli GF. Lipopolysaccharide-induced lung injury in mice. I. Concomitant evaluation of inflammatory cells and haemorrhagic lung damage. *Pulm Pharmacol Ther*. 2000;13(2):61–69. doi:10.1006/pupt.2000.0231
33. Beitler JR, Thompson BT, Baron RM, et al. Advancing precision medicine for acute respiratory distress syndrome. *Lancet Respir Med*. 2022;10(1):107–120. doi:10.1016/S2213-2600(21)00157-0
34. Kumar V. Pulmonary innate immune response determines the outcome of inflammation during pneumonia and sepsis-associated acute lung injury. *Front Immunol*. 2020;11:1722. doi:10.3389/fimmu.2020.01722
35. Fan E, Brodie D, Slutsky AS. Acute respiratory distress syndrome: advances in diagnosis and treatment. *JAMA*. 2018;319(7):698–710. doi:10.1001/jama.2017.21907
36. Huang Q, Le Y, Li S, Bian Y. Signaling pathways and potential therapeutic targets in acute respiratory distress syndrome (ARDS). *Respir Res*. 2024;25(1):30. doi:10.1186/s12931-024-02678-5
37. Qi W, Li H, Cai XH, et al. Lipoxin A4 activates alveolar epithelial sodium channel gamma via the microRNA-21/PTEN/AKT pathway in lipopolysaccharide-induced inflammatory lung injury. *Lab Invest*. 2015;95(11):1258–1268. doi:10.1038/labinvest.2015.109
38. Yang JX, Li M, Chen XO, et al. Lipoxin A(4) ameliorates lipopolysaccharide-induced lung injury through stimulating epithelial proliferation, reducing epithelial cell apoptosis and inhibits epithelial-mesenchymal transition. *Respir Res*. 2019;20(1):192. doi:10.1186/s12931-019-1158-z
39. Wang Q, Zheng X, Cheng Y, et al. Resolvin D1 stimulates alveolar fluid clearance through alveolar epithelial sodium channel, Na,K-ATPase via ALX/cAMP/PI3K pathway in lipopolysaccharide-induced acute lung injury. *J Immunol*. 2014;192(8):3765–3777. doi:10.4049/jimmunol.1302421
40. Sanchez-Garcia S, Jaen RI, Fernandez-Velasco M, Delgado C, Bosca L, Prieto P. Lipoxin-mediated signaling: ALX/FPR2 interaction and beyond. *Pharmacol Res*. 2023;197:106982. doi:10.1016/j.phrs.2023.106982
41. Qiao X, Yin J, Zheng Z, Li L, Feng X. Endothelial cell dynamics in sepsis-induced acute lung injury and acute respiratory distress syndrome: pathogenesis and therapeutic implications. *Cell Commun Signal*. 2024;22(1):241. doi:10.1186/s12964-024-01620-y
42. Suchitha GP, Devasahayam Arokia Balaya R, Prasad TSK, Dagamajalu S. A signaling network map of Lipoxin (LXA4): an anti-inflammatory molecule. *Inflamm Res*. 2024;73(7):1099–1106. doi:10.1007/s00011-024-01885-6
43. Wang J, Miao Z, Gao Y, Xie Z, Liu M, Zou W. Formyl peptide receptor 2: a potential therapeutic target for inflammation-related diseases. *Pharmacol Rep*. 2025;77(3):593–609. doi:10.1007/s43440-025-00704-x
44. Wiktorowska-Owczarek A, Berezinska M, Nowak JZ. PUFAs: structures, metabolism and functions. *Adv Clin Exp Med*. 2015;24(6):931–941. doi:10.17219/acem/31243
45. Lu W, Yao X, Ouyang P, et al. Drug repurposing of histone deacetylase inhibitors that alleviate neutrophilic inflammation in acute lung injury and idiopathic pulmonary fibrosis via inhibiting leukotriene A4 hydrolase and blocking LTB4 biosynthesis. *J Med Chem*. 2017;60(5):1817–1828. doi:10.1021/acs.jmedchem.6b01507
46. Dalli J, Colas RA, Quintana C, et al. Human sepsis eicosanoid and proresolving lipid mediator temporal profiles: correlations with survival and clinical outcomes. *Crit Care Med*. 2017;45(1):58–68. doi:10.1097/CCM.0000000000002014
47. Subramanian BC, Majumdar R, Parent CA. The role of the LTB(4)-BLT1 axis in chemotactic gradient sensing and directed leukocyte migration. *Semin Immunol*. 2017;33:16–29. doi:10.1016/j.smim.2017.07.002
48. He R, Chen Y, Cai Q. The role of the LTB4-BLT1 axis in health and disease. *Pharmacol Res*. 2020;158:104857. doi:10.1016/j.phrs.2020.104857
49. Basil MC, Levy BD. Specialized pro-resolving mediators: endogenous regulators of infection and inflammation. *Nat Rev Immunol*. 2016;16(1):51–67. doi:10.1038/nri.2015.4
50. Huang Y, Dong S, Zhang Y, et al. Electroacupuncture promotes resolution of inflammation by modulating SPMs via vagus nerve activation in LPS-induced ALI. *Int Immunopharmacol*. 2025;147:113941. doi:10.1016/j.intimp.2024.113941
51. Serhan CN, Brain SD, Buckley CD, et al. Resolution of inflammation: state of the art, definitions and terms. *FASEB J*. 2007;21(2):325–332. doi:10.1096/fj.06-7227rev
52. Sekheri M, El Kebir D, Edner N, Filep JG. 15-Epi-LXA(4) and 17-epi-RvD1 restore TLR9-mediated impaired neutrophil phagocytosis and accelerate resolution of lung inflammation. *Proc Natl Acad Sci U S A*. 2020;117(14):7971–7980. doi:10.1073/pnas.1920193117
53. Machado MG, Tavares LP, Souza GVS, et al. The Annexin A1/FPR2 pathway controls the inflammatory response and bacterial dissemination in experimental pneumococcal pneumonia. *FASEB J*. 2020;34(2):2749–2764. doi:10.1096/fj.201902172R
54. Zhu X, Guo Q, Zou J, et al. MiR-19a-3p suppresses M1 macrophage polarization by inhibiting STAT1/IRF1 pathway. *Front Pharmacol*. 2021;12:614044. doi:10.3389/fphar.2021.614044
55. Xia T, Zhang M, Lei W, et al. Advances in the role of STAT3 in macrophage polarization. *Front Immunol*. 2023;14:1160719. doi:10.3389/fimmu.2023.1160719
56. Maderna P, Cottell DC, Toivonen T, et al. FPR2/ALX receptor expression and internalization are critical for lipoxin A4 and annexin-derived peptide-stimulated phagocytosis. *FASEB J*. 2010;24(11):4240–4249. doi:10.1096/fj.10-159913
57. Lim EY, Lee SY, Shin HS, Kim GD. Reactive oxygen species and strategies for antioxidant intervention in acute respiratory distress syndrome. *Antioxidants*. 2023;12(11). doi:10.3390/antiox12112016
58. Ye W, Zheng C, Yu D, et al. Lipoxin A4 ameliorates acute pancreatitis-associated acute lung injury through the antioxidative and anti-inflammatory effects of the Nrf2 pathway. *Oxid Med Cell Longev*. 2019;2019:2197017. doi:10.1155/2019/2197017
59. He S, Shi J, Liu W, et al. Heme oxygenase-1 protects against endotoxin-induced acute lung injury depends on NAD(+)-mediated mitonuclear communication through PGC1alpha/PPARgamma signaling pathway. *Inflamm Res*. 2022;71(9):1095–1108. doi:10.1007/s00011-022-01605-y
60. Luo YY, Wu SH, Lu HY, et al. Lipoxin A4 attenuates hyperoxia-induced lung epithelial cell injury via the upregulation of heme oxygenase-1 and inhibition of proinflammatory cytokines. *Mol Med Rep*. 2020;21(1):429–437. doi:10.3892/mmr.2019.10821
61. Cioccari L, Luethi N, Masoodi M. Lipid mediators in critically ill patients: a step towards precision medicine. *Front Immunol*. 2020;11:599853. doi:10.3389/fimmu.2020.599853

62. Maciuszek M, Cacace A, Brennan E, Godson C, Chapman TM. Recent advances in the design and development of formyl peptide receptor 2 (FPR2/ALX) agonists as pro-resolving agents with diverse therapeutic potential. *Eur J Med Chem*. 2021;213:113167. doi:10.1016/j.ejmech.2021.113167
63. McGuffee RM, Luetzen MA, Ford DA. Resolving lipoxin A(4): endogenous mediator or exogenous anti-inflammatory agent? *J Lipid Res*. 2025;66(2):100734. doi:10.1016/j.jlr.2024.100734
64. Jiao Y, Zhang T, Liu M, et al. Exosomal PGE2 from M2 macrophages inhibits neutrophil recruitment and NET formation through lipid mediator class switching in sepsis. *J Biomed Sci*. 2023;30(1):62. doi:10.1186/s12929-023-00957-9
65. Flerlage T, Crawford JC, Allen EK, et al. Single cell transcriptomics identifies distinct profiles in pediatric acute respiratory distress syndrome. *Nat Commun*. 2023;14(1):3870. doi:10.1038/s41467-023-39593-0
66. Duggal A, Camporota L. Sequencing interventions in ARDS: the critical role of timing and order in standardized management. *Intensive Care Med*. 2024;50(7):1133–1136. doi:10.1007/s00134-024-07412-9